

Boosting neutrino mass ordering sensitivity with inelasticity for atmospheric neutrino oscillation measurement

Santiago Giner Olavarrieta^{1,*}, Miaochen Jin (靳淼辰)^{1,†}, Carlos A. Argüelles^{1,‡},
Pablo Fernández^{2,§} and Ivan Martinez-Soler^{3,||}

¹*Department of Physics and Laboratory for Particle Physics and Cosmology,
Harvard University, Cambridge, Massachusetts 02138, USA*

²*Donostia International Physics Center DIPC, San Sebastián/Donostia, E-20018, Spain*

³*Department of Physics and Institute for Particle Physics Phenomenology,
University of Durham, Durham, DH1 3LE, United Kingdom*

 (Received 7 March 2024; accepted 28 August 2024; published 30 September 2024)

In this letter, we study the potential of boosting the atmospheric neutrino experiments sensitivity to the neutrino mass ordering (NMO) sensitivity by incorporating inelasticity measurements. We show how this observable improves the sensitivity to the NMO and the precision of other neutrino oscillation parameters relevant to atmospheric neutrinos, specifically in the IceCube-Upgrade and KM3NeT-ORCA detectors. Our results indicate that an oscillation analysis of atmospheric neutrinos, including inelasticity information, has the potential to enhance the ordering discrimination by several units of χ^2 in the assumed scenario of five and three years of running of IceCube-Upgrade and KM3NeT-ORCA detectors, respectively.

DOI: [10.1103/PhysRevD.110.L051101](https://doi.org/10.1103/PhysRevD.110.L051101)

Introduction. Unmagnetized neutrino experiments cannot distinguish neutrinos from antineutrinos on an event-by-event basis when studying neutrino-nucleon interactions. Instead, experiments operating without a magnet need to rely on the particle content of the beam or the use of kinematic observables to statistically separate neutrinos from antineutrinos. So far, analyses of atmospheric neutrinos aimed to determine neutrino oscillation parameters [1–4] have not exploited kinematic variables aimed at distinguishing between neutrinos and antineutrinos in large telescopes based on water/ice-Cherenkov.

This missing information undoubtedly hides the potential of atmospheric neutrinos in measuring the different oscillation effects that are distinct between neutrinos and antineutrinos, namely the mass ordering through the Mikheyev-Smirnov-Wolfenstein (MSW) [5,6] Earth

matter effects¹ and the magnitude of the CP -violating phase in the lepton sector [8]. This is particularly important since, as recently demonstrated in Ref. [9], atmospheric neutrino experiments are expected to yield one of the most precise measurements of the neutrino oscillation parameters and are expected to determine the neutrino mass ordering by the end of the decade.

With this motivation, the Super-Kamiokande experiment has already implemented various techniques to distinguish neutrinos from antineutrinos [10,11]; namely, detecting low-energy secondary particles like Michel electrons or neutrons and computing kinematically relevant variables when possible, that is, in the multi-ring samples. These features have already been included in previous sensitivity studies and also apply to the Hyper-Kamiokande experiment, therefore we shall exclude them in this study and focus on the improvements that inelasticity would bring to IceCube and ORCA oscillation analyses.

The former requires a low-background detector with very high photo-sensor coverage, which is currently out of reach for the large, next-generation, multi-megatonne neutrino detectors. On the other hand, in this work, we demonstrate how the IceCube-Upgrade and KM3NeT-ORCA detectors could use the reconstructed inelasticity of the neutrino interaction to improve the sensitivity to

*Contact author: santiagoginer@college.harvard.edu

†Contact author: miaochenjin@g.harvard.edu

‡Contact author: carguelles@fas.harvard.edu

§Contact author: pablo.fernandez@dipc.org

||Contact author: ivan.j.martinez-soler@durham.ac.uk

Published by the American Physical Society under the terms of the Creative Commons Attribution 4.0 International license. Further distribution of this work must maintain attribution to the author(s) and the published article's title, journal citation, and DOI. Funded by SCOAP³.

¹Alongside atmospheric neutrino experiments, long-baseline experiments like DUNE [7], we will also utilize matter effects to resolve the mass ordering.

neutrino mass ordering and the CP phase. The inelasticity y , also known as Bjorken- y , is the fraction of the neutrino energy transferred to a hadronic system with which the neutrino interacts. There are some efforts that has already been taken in the IceCube collaboration in reconstructing the inelasticity of low energy events [12]. Thus, in this letter, we extend the work in Ref. [9] by studying the impact in sensitivity of the IceCube-Upgrade and KM3NeT-ORCA neutrino telescopes that comes from incorporating an event's inelasticity in the oscillation analysis.

The results obtained in this work further complement the motivation of a combined oscillation analysis of atmospheric neutrinos to provide a precise picture of the mixing scenario independent from the current and early measurements of the next-generation accelerator experiments. Furthermore, our results motivate the development of techniques that enable the reconstruction of the inelasticity in neutrino telescopes.

Atmospheric neutrinos and antineutrinos. The study of neutrino oscillations has entered an era of high precision, where only a few aspects remain unknown. Among these unknowns are the octant of the θ_{23} , the mass ordering, and the CP -phase, δ_{CP} . Both the mass ordering and δ_{CP} predict different behaviors for neutrinos and antineutrinos as they propagate through Earth. Specifically, in the case of normal mass ordering (NO), where $m_3 > m_2, m_1$, a matter-induced resonance is predicted for neutrinos crossing the mantle and the core of the Earth at energies around 6 GeV. In the case of inverted ordering (IO), where $m_3 < m_1, m_2$, this resonance occurs in the antineutrino propagation, as illustrated in Fig. 1. A similar situation arises in the case of δ_{CP} , where, in the presence of CP -violation, the oscillation evolution differs between neutrinos and antineutrinos. For a detailed description of the effects of CP -violation on atmospheric neutrino evolution, see [9].

The different oscillation patterns between neutrinos and antineutrinos suggest that the separation of both particle types in the event basis is the best way to explore the aforementioned parameters. In accelerator experiments, this is done by running the experiment in both the neutrino and antineutrino modes, while in the case of atmospheric neutrinos, the flux contains both neutrino types. Therefore, we look for an alternative way to discriminate between neutrino- and antineutrino-type events.

Following a neutrino's charged-current (CC) interaction with a nucleon (N), the neutrino energy is split between the leptonic (l_α) and hadronic (h) currents, $\nu_\alpha + N \rightarrow l_\alpha + h$. The $V - A$ structure of the weak tensor in the case of the neutrino interaction results into a different cross section for neutrinos and antineutrinos [14], when neutrinos interact primarily with valence quarks, which is the case at the relevant energies. Considering just the case where the neutrinos interact via deep-inelastic scattering (DIS), the relevant component above 3 GeV, and

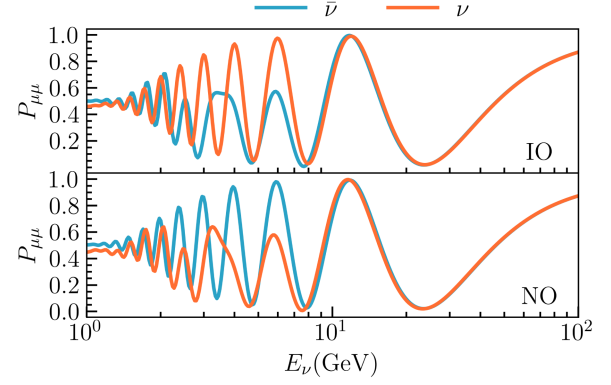


FIG. 1. Muon disappearance probabilities for both mass orderings, normal (NO) and inverted (IO), and both neutrinos and antineutrino, considering a trajectory crossing the entire Earth ($\cos \theta_\nu = -0.95$). We used the results of the latest global analysis [13] for the best-fit values of the parameters. A Gaussian filter with a width of $5\% \sqrt{E_\nu}$ has been included to remove the fast oscillations at lower energies.

following the notation in [15], the neutrino cross section can be written in terms of the inelasticity ($y = 1 - E_l/E_\nu$), where E_l is the energy of the outgoing lepton, and the Bjorken scaling variable (x) as

$$\frac{d\sigma_\nu^{CC}}{dydx} = \frac{G_F^2 xs}{2\pi} (Q(x) + \bar{Q}(x) \times (1 - y)^2), \quad (1)$$

$$\frac{d\sigma_{\bar{\nu}}^{CC}}{dydx} = \frac{G_F^2 xs}{2\pi} (\bar{Q}(x) + Q(x) \times (1 - y)^2), \quad (2)$$

where G_F is the Fermi constant and s is the square of the center-of-mass energy. The symbols $Q(x)$ and $\bar{Q}(x)$ corresponds to the sum of all the parton distribution functions (PDFs) for quarks and antiquarks that contribute to the nucleons. To explore the dependence of the neutrino cross section on the inelasticity, we have integrated the double differential cross section over x within the kinematic allowed region, and using the PDF4LHC21 set [16] PDFs set. We find an almost uniform energy distribution of the outgoing lepton in the case of the neutrino interaction, as shown in Fig. 2. In the case of the antineutrino interaction, most of the energy of the incoming neutrino is carried out by the outgoing lepton. Therefore, it is possible to get a large neutrino-antineutrino separation for large values of y .

Although we have restricted the discussion in this section to the DIS interaction, all the results that are presented in this analysis are based on simulations that includes all the interaction channels, as described in [9].

Experiments and methods. The IceCube Neutrino Observatory [17] is an ice-Cherenkov neutrino detector located on average 2 km below the surface at the geographic South Pole. It consists of 5160 light sensors known

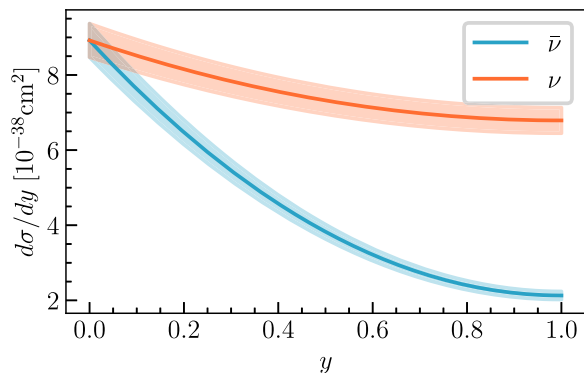


FIG. 2. Differential neutrino charge current cross section for the DIS regime. The shaded region corresponds to the 1σ uncertainty region included for DIS in this analysis.

as digital optical modules (DOMs) that allow it to detect neutrino interactions above ~ 10 GeV. Depending on the type of particle propagating through the ice, an event will correspond to one of two possible morphologies, namely, *tracks*, coming from the propagation of muons, and *cascades*, coming from the propagation of electrons, taus, and/or hadronic or electromagnetic cascades. In the near future, IceCube will undergo an upgrade [18,19] consisting of deploying additional strings in order to lower the energy threshold to a few GeV.

We further consider the ORCA detector, which is part of the KM3NeT water-Cherenkov neutrino telescope currently under construction in the Mediterranean Sea [20]. As in the case of IceCube, ORCA also identifies tracks and cascades as possible event morphologies, but have also developed a third sample, namely, the *intermediate*, for events that cannot be clearly identified as part of the former two. For the purposes of our analysis, we use the open-access Monte Carlo simulation of ORCA developed in [9], which is built as an extension of the open-access IceCube-Upgrade Monte Carlo release.

In both experiments, we compute the inelasticity for charged-current ν_μ events which produce an outgoing muon, reconstructed as a track, and a hadronic shower, identified as a cascade. In terms of reconstructed quantities,

$$y_r = \frac{E_r^{\text{casc}}}{E_r^{\text{casc}} + E_r^{\text{track}}}. \quad (3)$$

Current oscillation analysis carried away by IceCube and ORCA use a two-dimensional histogram of the events in terms of the reconstructed energy and the direction for each morphological category. To incorporate the inelasticity in the analysis, we modified the Monte Carlo simulations for IceCube-Upgrade [21,22] and ORCA by adding a variable corresponding to the reconstructed inelasticity, y_r . For every MC event reconstructed as a track, we generate a set of N additional events, where the inelasticity is reconstructed based on the reconstructed energy for the

track and the cascade. For the main results of this work, we have assumed a Gaussian distribution with uncertainty of $\sigma_T = 20\%$ for tracks and $\sigma_C = 30\%$ for cascades [4]. For the purposes of this letter, we used the case of $N = 20$ for the IceCube simulation and $N = 10$ for ORCA.²

In addition to the binning scheme described in [9], a third dimension is implemented for track events of both experiments, including 10 bins for the reconstructed inelasticity. An example of the event distribution we predict is shown in Fig. 3, where we have chosen one bin in zenith $\cos\theta_r \in [-0.8, -0.6]$ and energy $E_r \in [5.0, 6.3]$ GeV. As anticipated from the previous discussion, for large values of y , the event distribution is primarily dominated by the neutrino sample. In the case of antineutrinos, the event distribution is concentrated in the bins with small y_r . The event distribution is depicted for both mass orderings, normal (solid), and inverted (dash). For neutrinos, the different mass orderings lead to deviations in the event distribution which are almost uniform in y_r . For the case of antineutrino, this deviation concentrates at lower y_r .

Analysis and results. We have investigated how the sensitivity to oscillation parameters improves with the inclusion of inelasticity in the analysis. Through a combined analysis using currently publicly available IceCube-Upgrade and ORCA simulations, we have explored the sensitivity to the less constrained oscillation parameters— Δm_{31}^2 , mass ordering, and the CP -phase. Since atmospheric neutrino experiments are not sensitive to the solar parameters, Δm_{21}^2 and $\sin^2\theta_{12}$, we have fixed both of these as well as the reactor angle, $\sin^2\theta_{13}$, to their best-fit values [13].³ Regarding systematic uncertainties, we have taken into account uncertainties associated with the atmospheric neutrino flux, neutrino cross section, and detector response. These uncertainties have been included in the analysis in a manner similar to that presented in [9].

The main results of the combined analysis are illustrated in Fig. 4. The sensitivity shown in the figure corresponds to the combination of IceCube-Upgrade and ORCA, with exposures of 5 and 3 years, respectively. In both figures, we assume normal ordering as the benchmark scenario. Regarding $|\Delta m_{31}^2|$, we observed an improvement of more than 30%, achieving a precision below the percent level (0.7%), as depicted in Fig. 4 (left, solid lines). However, for $\sin^2\theta_{23}$, which is influenced by the neutrino angular

²We explored the sensitivity considering different values for N between $N = 10$ and $N = 100$, finding no significant deviation of the results.

³We have explore how the sensitivity to the mass ordering and the CP -phases changes with and without the present constraints of the solar parameters and θ_{13} . Our results indicate that Δm_{21}^2 and θ_{12} do not have any impact on the mass ordering or δ_{CP} . In the case of θ_{13} , the current sensitivity from reactor experiments is enough to reach 7σ in the mass order, and it does not have a large impact over δ_{CP} .

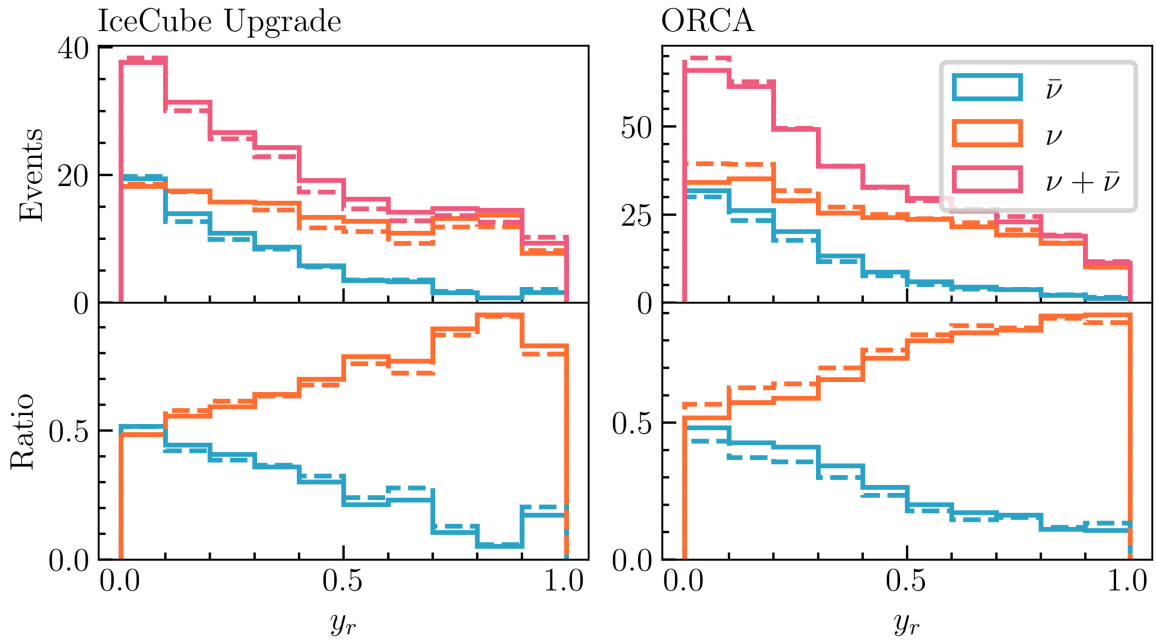


FIG. 3. Histogram of events in IceCube Upgrade and ORCA as a function of y_r for a bin in $E_r \in [5.0, 6.3]$ GeV and $\cos \theta_r \in [-0.8, -0.6]$. The solid line corresponds to Normal Ordering and the dashed line to Inverted Ordering. In the lower panel, we display the ratio between the neutrinos (orange) and antineutrinos (blue) and the total number of events for both normal and inverted ordering.

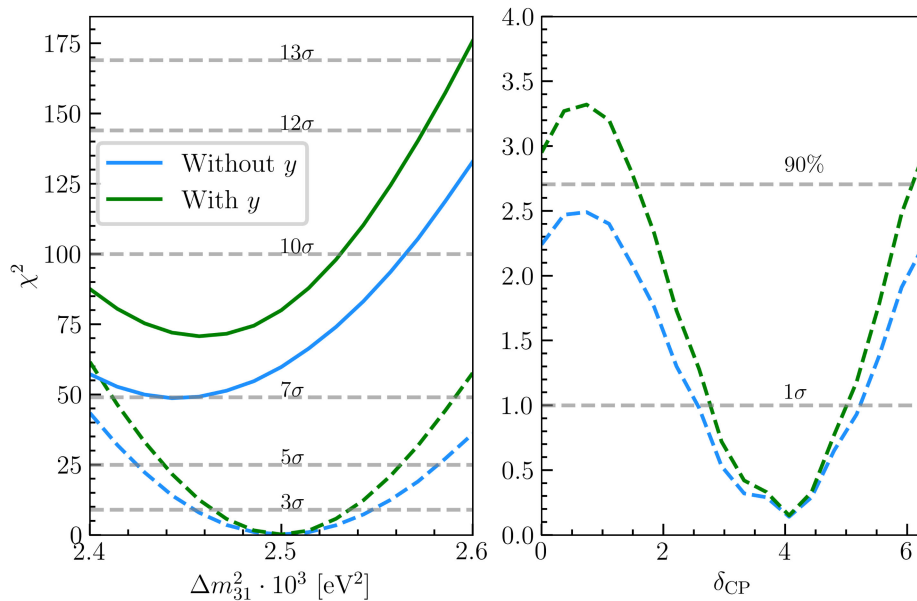


FIG. 4. Left: sensitivity from the combined analysis of IceCube-Upgrade (5 years) and ORCA (3 years) to Δm_{31}^2 (solid lines) incorporating y binning (green) and the usual analysis (blue), assuming true normal ordering. Dashed lines are the inverted ordering fit, showing the NMO sensitivity in units of χ^2 . Right: combined sensitivity to δ_{CP} incorporating the y (green) and the usual analysis (blue), assuming true normal ordering.

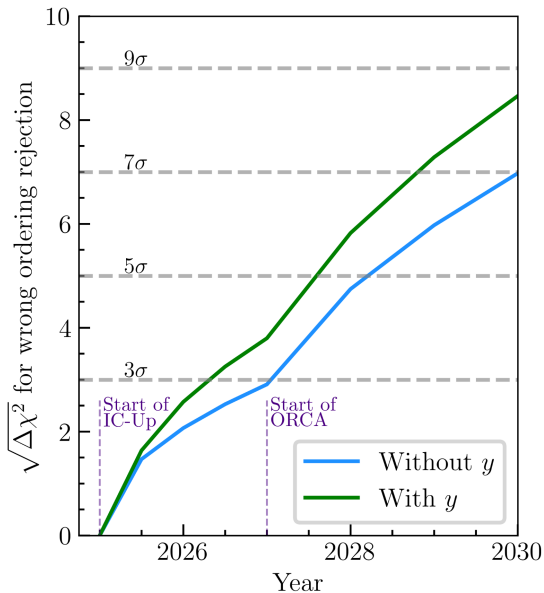


FIG. 5. Combined neutrino mass ordering sensitivity in units of $\sqrt{\Delta\chi^2}$ as a function of years in operation of both IceCube-Upgrade and ORCA.

resolution, no improvement is observed. For both parameters, profiling has been performed over δ_{CP} and the parameters not shown.

The sensitivity to the ordering is depicted on the right panel of Fig. 4 by the dashed lines. We fit the event distribution assuming inverted ordering to the normal ordering scenario. We also take $\delta_{CP} = 4.082$ as the best-fit value [13]. The combination of IceCube Upgrade and ORCA will enable us to predict a 7σ exclusion of the inverted ordering without including the inelasticity, as shown in [9]. With the inclusion of inelasticity in the analysis, the sensitivity increases to $\sim 8.4\sigma$. When considering each experiment separately, IceCube Upgrade can reach $\sim 5\sigma$ in 3.5 yr, while ORCA can do it in 2.5 yr. The different best-fit values found for Δm_{31}^2 in NMO and IMO correspond to the phase difference between the two mass orderings. Additionally, Fig. 5 showcases the improvement gained from including the inelasticity in the event analysis as a function of years in operation of both experiments.

Finally, in the context of the CP -violating phase, although it does not have a significant impact on the muon disappearance channel [23], the inclusion of inelasticity in the analysis increases the resolution of δ_{CP} by $\sim 15\%$.

Furthermore, to assess the resilience of our results, we investigated how the new sensitivity changes under limitations related to energy reconstruction and the possible misclassification of events with large inelasticity. These tests confirmed the robustness of our method to these potential errors; refer to the Supplemental Material [24] for detailed information.

Conclusion. In this letter, we introduced a novel approach to the oscillation analysis of the atmospheric neutrino data suitable for the upcoming IceCube-Upgrade and ORCA experiments. We motivate and demonstrate that introducing the information of the reconstructed inelasticity of track events has the potential to discern neutrinos and antineutrinos in the few GeV region, thus impacting the sensitivity of the relevant oscillation parameters, namely the neutrino mass ordering, the squared-mass difference and the CP -phase. These results motivate the development of reconstruction techniques that can infer the inelasticity for sub-100 GeV energies.

This work builds up the results from Ref. [9], showing the relevant role of atmospheric neutrinos in unequivocal measuring the neutrino mass ordering before the end of the decade. Additionally, they will constrain the allowed values for the remaining oscillation parameters independently from the long-baseline programs, which will carry a precise determination of parameters such as δ_{CP} and $\sin\theta_{23}$. The different sensitivity to various oscillation parameters between reactor, solar, accelerator, and atmospheric neutrino experiments supports the usefulness of combined analysis that exploits their distinct sensitivity coverage. In this context, our letter's conclusions further motivate the inclusion of neutrino telescope atmospheric neutrino measurements in the global effort to determine neutrino oscillation parameters.

Acknowledgments. S. G. O. acknowledges support from the Harvard College Research Program. C. A. A. is supported by the Faculty of Arts and Sciences of Harvard University, the National Science Foundation, IAIFI, and the David & Lucile Packard Foundation. C. A. A. and I. M. S. were supported by the Alfred P. Sloan Foundation for part of this work. M. J. is supported by the National Science Foundation and the Faculty of Arts and Sciences of Harvard University. I. M. S. is supported by STFC Grant No. ST/T001011/1.

- [1] K. Abe *et al.* (Super-Kamiokande Collaboration), Atmospheric neutrino oscillation analysis with external constraints in Super-Kamiokande I-IV, *Phys. Rev. D* **97**, 072001 (2018).
- [2] A. Albert *et al.* (ANTARES Collaboration), Measuring the atmospheric neutrino oscillation parameters and constraining the 3 + 1 neutrino model with ten years of ANTARES data, *J. High Energy Phys.* **06** (2019) 113.
- [3] V. Pestel, L. Nauta, and Z. Aly (KM3NeT Collaboration), First neutrino oscillation measurement with KM3NeT/ORCA, *Proc. Sci. NuFact2021* (2022) 064.
- [4] R. Abbasi *et al.* (IceCube Collaboration), Measurement of atmospheric neutrino mixing with improved IceCube DeepCore calibration and data processing, *Phys. Rev. D* **108**, 012014 (2023).
- [5] L. Wolfenstein, Neutrino oscillations in matter, *Phys. Rev. D* **17**, 2369 (1978).
- [6] S. P. Mikheyev and A. Y. Smirnov, Resonance amplification of oscillations in matter and spectroscopy of solar neutrinos, *Sov. J. Nucl. Phys.* **42**, 913 (1985).
- [7] B. Abi *et al.* (DUNE Collaboration), Deep Underground Neutrino Experiment (DUNE), far detector technical design report, Volume II: DUNE physics, [arXiv:2002.03005](https://arxiv.org/abs/2002.03005).
- [8] S. Razzaque and A. Y. Smirnov, Super-PINGU for measurement of the leptonic CP -phase with atmospheric neutrinos, *J. High Energy Phys.* **05** (2015) 139.
- [9] C. A. Argüelles, P. Fernández, I. Martínez-Soler, and M. Jin, Measuring oscillations with a million atmospheric neutrinos, *Phys. Rev. X* **13**, 041055 (2023).
- [10] K. Abe *et al.* (Super-Kamiokande Collaboration), Neutron tagging following atmospheric neutrino events in a water Cherenkov detector, *J. Instrum.* **17**, P10029 (2022).
- [11] T. Wester *et al.* (Super-Kamiokande Collaboration), Atmospheric neutrino oscillation analysis with neutron tagging and an expanded fiducial volume in Super-Kamiokande I-V, *Phys. Rev. D* **109**, 072014 (2024).
- [12] J. H. Peterson, M. P. Rodriguez, and K. Hanson (IceCube Collaboration), 2D convolutional neural network for event reconstruction in IceCube DeepCore, *Proc. Sci. ICRC2023* (2023) 1129 [[arXiv:2307.16373](https://arxiv.org/abs/2307.16373)].
- [13] I. Esteban, M. C. Gonzalez-Garcia, M. Maltoni, T. Schwetz, and A. Zhou, The fate of hints: Updated global analysis of three-flavor neutrino oscillations, *J. High Energy Phys.* **09** (2020) 178.
- [14] M. Ribordy and A. Y. Smirnov, Improving the neutrino mass hierarchy identification with inelasticity measurement in PINGU and ORCA, *Phys. Rev. D* **87**, 113007 (2013).
- [15] F. Halzen and A. D. Martin, *Quarks and Leptons: An Introductory Course in Modern Particle Physics* (1984).
- [16] R. D. Ball *et al.* (PDF4LHC Working Group Collaboration), The PDF4LHC21 combination of global PDF fits for the LHC Run III, *J. Phys. G* **49**, 080501 (2022).
- [17] A. Achterberg *et al.* (IceCube Collaboration), First year performance of the IceCube neutrino telescope, *Astropart. Phys.* **26**, 155 (2006).
- [18] A. Ishihara (IceCube Collaboration), The IceCube upgrade—design and science goals, *Proc. Sci. ICRC2019* (2021) 1031 [[arXiv:1908.09441](https://arxiv.org/abs/1908.09441)].
- [19] T. Stuttard (IceCube Collaboration), Neutrino oscillations and PMNS unitarity with IceCube/DeepCore and the IceCube upgrade, *Proc. Sci. NuFact2019* (2020) 099.
- [20] S. Adrián-Martínez *et al.* (KM3Net Collaboration), Letter of intent for KM3NeT 2.0, *J. Phys. G* **43**, 084001 (2016).
- [21] IceCube Collaboration, IceCube: Upgrade neutrino Monte Carlo simulation (2020), [10.21234/qfz1-yh02](https://arxiv.org/abs/10.21234/qfz1-yh02).
- [22] P. Fernandez, I. Martínez-Soler, C. A. Argüelles, and J. Miaochen, Atmospheric Neutrino Monte Carlo Simulations (Harvard Dataverse, 2023), [10.7910/DVN/OS5N7U](https://doi.org/10.7910/DVN/OS5N7U).
- [23] P. B. Denton, CP -violation with neutrino disappearance, *Phys. Rev. Lett.* **133**, 031801 (2024).
- [24] See Supplemental Material at <http://link.aps.org/supplemental/10.1103/PhysRevD.110.L051101>, we explore the uncertainties associated with inelasticity and their impact on determining the oscillation parameters.